Available online at www.sciencedirect.com
ScienceDirect
Bioorganic & Medicinal Chemistry 15 (2007) 186–193
Bioorganic & Medicinal Chemistry

Synthesis of a non-cationic, water-soluble perylenetetracarboxylic diimide and its interactions with G-quadruplex-forming DNA

Ramakrishna Samudrala, Xu Zhang, Randy M. Wadkins and Daniell Lewis Mattern*

Department of Chemistry and Biochemistry, Box 1848, University of Mississippi University, MS 38677, USA

Received 27 July 2006; revised 27 September 2006; accepted 29 September 2006
Available online 10 October 2006

Abstract—A number of *N*,*N*′-disubstituted perylenetetracarboxylic diimides have been reported to bind effectively to DNA that adopts G-quadruplex motifs. In some cases, this binding may actively drive the transition from single-strand DNA to the quadruplex form. The perylenediimides in the reported cases all have amine-containing side chains, which are thought to interact with the grooves of the quadruplex and help dictate the selectivity of these compounds for quadruplex versus duplex DNA. We synthesized a polyethyleneglycol-swallowtailed (PEG-tailed) perylenediimide that is water-soluble even though it is uncharged. Binding to duplex and quadruplex DNA of this perylenediimide was studied by fluorescence quenching titrations under a variety of salt conditions, and the compound's effect on quadruplex formation was studied by non-denaturing gel electrophoresis. Our results indicate that while the molecule binds to single-stranded DNA quite effectively and with selectivity, it does not drive the transition of the DNA to the tetrameric quadruplex structure, supporting the idea that charge neutralization is a key component of perylene compounds that stabilize tetrameric quadruplexes.

1. Introduction

It is now well established that guanine-rich sequences of DNA can adopt secondary structures quite distinct from typical Watson-Crick duplex DNA. These secondary structures include 'frayed wires'[1] and quadruplex DNA.[2,3] Quadruplexes are of particular interest in cancer biology as they are thought to play a role in the stabilization of telomeric DNA and its binding to the enzyme telomerase, which is active in a number of tumor types.[4,5] Consequently, agents that target telomeric quadruplexes are thought to be potential antitumor agents.[6,7] More recently, quadruplexes have also been identified in promoters of specific genes, notably c-MYC,[8–10] and agents that bind quadruplex DNA can affect transcription of genes regulated by these promoters.

Although a number of different small molecules are known to interact with quadruplex DNA, the most often studied are those that are derivatives of porphyrin and perylene. The perylenediimide PIPER (**1**) has been shown to promote formation of quadruplex DNA from single strands.[11] A number of other perylenediimides bind to quadruplex DNA, and their affinities are controlled by the structures of the side chains attached to the imide nitrogens. The side chains examined have all contained cationic amino moieties under the conditions studied, and these groups are thought to control specificity for quadruplex versus duplex DNA binding.[12,13] We are unaware of any reports on non-cationic perylenes binding to quadruplex DNA, although the compound PIPER2 (**2**), containing a 2-pyridino side chain, has only a small fractional charge at pH 7 and above.[12] Disinterest in uncharged perylenediimides is likely due to the extremely poor solubility of most substituted perylenediimides in aqueous solutions.

Recently, Wescott and Mattern[14] described the synthesis of a series of perylenediimides substituted with a 19-carbon 'swallowtail' (a long alkyl group connected at the middle of its chain[15]) on one of the imide nitrogens, and a variety of one-electron donor groups on the other nitrogen. These materials were prepared to test their ability to rectify electrical current when aligned in a monolayer[16] utilizing the electron-acceptor character of perylenediimides. Swallowtails (as in **3**) are crucial for imparting workable solubility to perylenediimides in nonpolar solvents. In polar solvents like alcohol or water, however, the solubility of alkyl-swallowtailed

* Corresponding author. Tel.: +1 662 915 5335; fax: +1 662 915 7300; e-mail: mattern@olemiss.edu

0968-0896/$ - see front matter © 2006 Elsevier Ltd. All rights reserved.
doi:10.1016/j.bmc.2006.09.075

perylenediimides is negligible. We anticipated that development of a hydrophilic swallowtail would be advantageous for eventual control of rectifier orientation. Perylenediimides that contain long polyethylene glycol (PEG) swallowtails[17] or shorter PEG segments separated from the imide nitrogen by three-carbon spacers like **4**[18] have good water solubility, and suggested that perylenediimide **5** with two PEG swallowtails would be soluble in polar solvents. We report here the synthesis of **5** and its aqueous solubility. With **5** in hand, its interaction with DNA in aqueous solutions could be readily investigated, allowing observation of the effect of uncharged perylenediimides on the formation of quadruplex DNA, which is the focus of this report. To our knowledge, **5** is the first water-soluble perylenediimide that does not contain an amino-substituted side chain to be examined for its interaction with DNA.

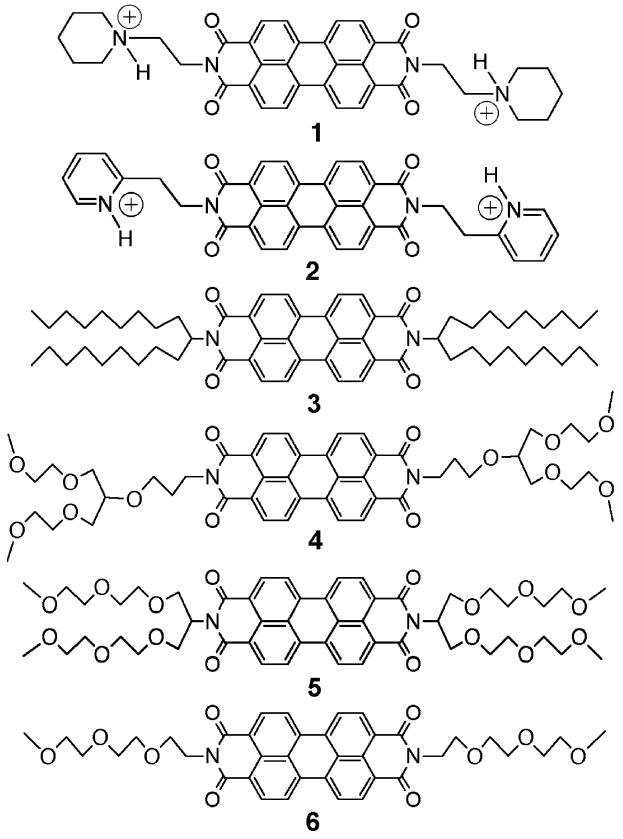

2. Results and discussion

2.1. Synthesis

Perylenediimides are constructed by reacting perylenetetracarboxylic dianhydride (**7**) with an appropriate 1° amine[19] (Scheme 1). The polyether 1° amine 10-amino-2,5,8,12,15,18-hexaoxanonadecane (**9**) was therefore a key intermediate for the synthesis of **5**. The reaction of serinol (**10**) with benzyl bromide and K_2CO_3 in ethanol[20] gave dibenzylserinol (**11**),[21] which was treated with NaH and the PEG tosylate **13**.[22] The resulting double Williamson alkylation[22] gave the protected PEG-amine **14**. Deprotection to **9** was accomplished by catalytic hydrogenation using a large excess of Pd/C. (Similar attempts to prepare **9** using single *t*-Boc[23] and CBZ[24] protection of the amino group were unsuccessful.) The resulting amine (**9**) was condensed with **7** in molten imidazole with zinc acetate[25] to give the crude target **5** (Scheme 2).

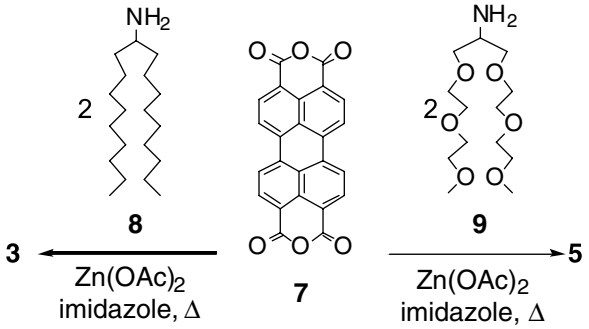

Scheme 1.

Purification of the doubly PEG-swallowtailed **5** was performed by exploiting the basicity of imidazole with an acidic ion exchange chromatographic separation. After rinsing the column with HCl (aq), elution of the reaction mixture (acidified with AcOH) with methanol afforded **5** free from imidazole. This material could be further purified by column chromatography (basic alumina, 0.4–0.8% MeOH in EtOAc). Compound **5** was found to be highly soluble in water, methanol, chloroform, and ethyl acetate, giving deep red solutions in each. Less solubility was observed in diethyl ether (Et_2O/H_2O partition ratio by UV–visible absorbance = 1:7) and no solubility was observed in hexane. Because of the high solubility of **5** in water

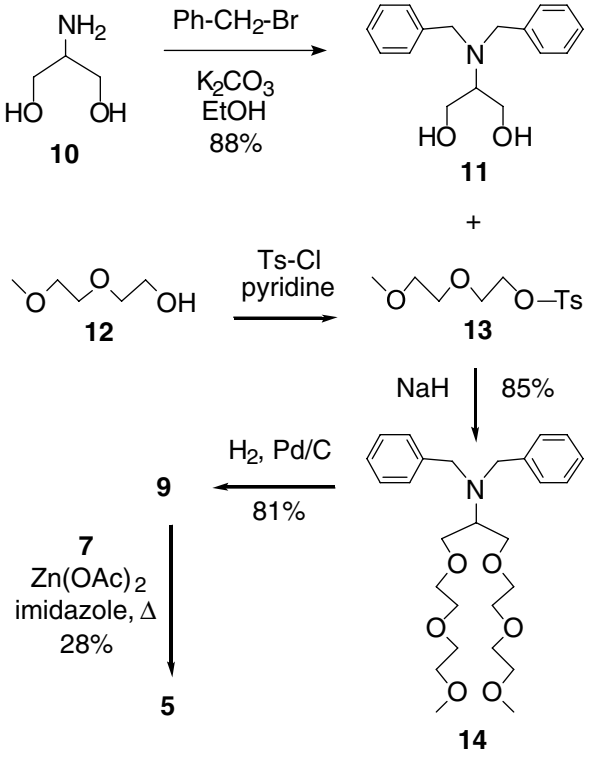

Scheme 2.

and other solvents, and the small amounts accessible by synthesis, we were unable to saturate enough solution to determine its maximal solubility.

We also prepared **6**, a perylenediimide with two short unbranched PEG tails, to compare with **5**. The Mitsunobu reaction of alcohol **15** with phthalimide, DIAD, and PPh_3 gave *N*-(3,6,9-trioxadecyl)phthalimide (**16**), which afforded **17** upon hydrazinolysis, as described by Dombi et al.[26] Coupling of **17** with **7** gave $CHCl_3$-soluble **6**.[17] Assuming a molar absorptivity comparable to that of **5** (*vide infra*), we estimate the solubility of **6** in water as 13 mM. However, **6** was substantially less soluble in buffers containing 100 mM KCl, and precipitation of this compound in buffers made it undesirable for studies of its DNA-binding abilities (Scheme 3).

The solubility of **5** and **6** allowed us to compare their UV–visible spectra in a range of solvents ($CHCl_3$, Et_2O, CH_3OH, and H_2O), as shown in Figure 1 and Table 1. The spectra were similar in the organic solvents, resembling that of alkyl-swallowtailed perylenediimides like **3** in $CHCl_3$.[27] However, solvatochromism was observed for **5** in water, as shown by a decreased extinction coefficient and a bathochromic shift of absorption peaks. Furthermore, the relative intensities of the absorption peaks changed, with the $0 \rightarrow 1$ transition (at 501 nm) becoming λ_{max}. Similar behavior has been reported for tethered oligomers of perylenediimides as well as for concentrated solutions of perylenediimides,[28,29] suggesting that **5** in water forms aggregates at concentrations ~1 mM where solutions of perylenediimides in nonpolar solvents are monomeric.[28,29] As aggregation of perylenediimides is important for quadruplex stabilization,[11,13] the pH-independent aggregation may prove important for the interaction of non-cationic pereylenediimides with DNA. The UV–visible spectra of **6** in chloroform and water (Fig. 1) are similar to those of **5**, although the absorptions in water are not as well resolved. Both compounds also exhibited intense fluorescence emission (described below for **5**).

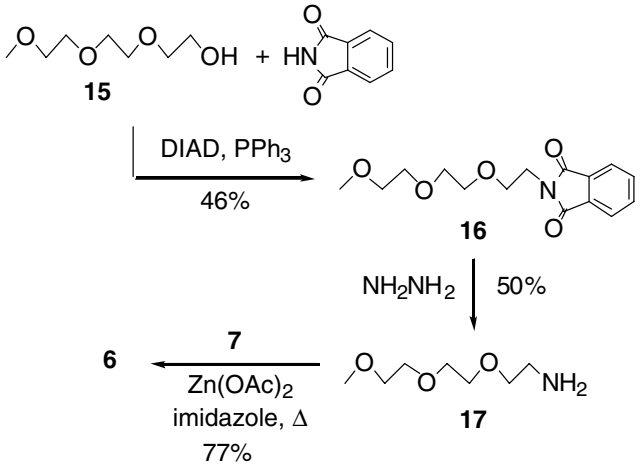

Scheme 3.

Table 1. UV–visible absorption maxima and molar absorptivities of **5** in various solvents

	λ_1	λ_2	λ_3	ε (λ_{max})
Et_2O	452	482	**517**	6.5×10^4
MeOH	457	486	**521**	6.8×10^4
$CHCl_3$	458	489	**525**	8.2×10^4
H_2O	472	**501**	539	2.4×10^4

λ_{max} values (nm) are in bold.

2.2. Titration curves

We investigated the ability of **5** to bind to DNA. For comparison, we used PIPER[11] (**1**; a kind gift of Sean

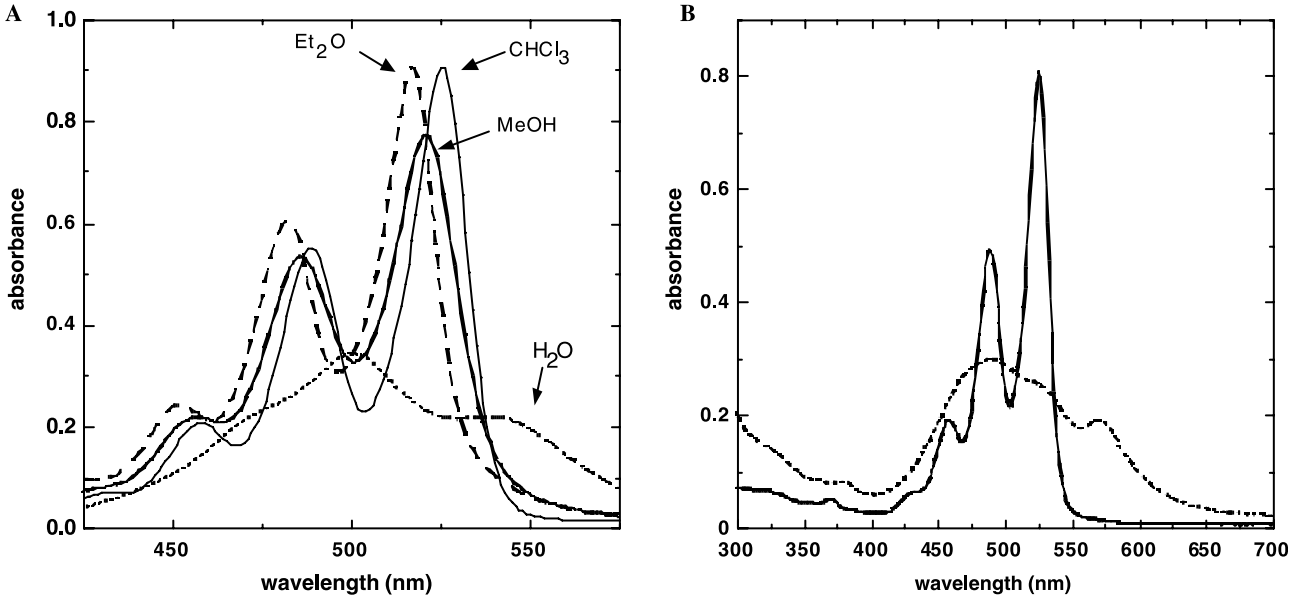

Figure 1. (A) UV–visible absorption spectra of **5** in various solvents: H_2O, 43 μM; methanol (MeOH), 42 μM; diethyl ether (Et_2O), 49 μM; $CHCl_3$, 38 μM. (B) UV–visible absorption spectra of **6** in $CHCl_3$ and H_2O. The sample in water is saturated (ca. 13 mM).

M. Kerwin, University of Texas). The two synthetic DNA sequences used were the G-rich ssDNAs taken from the human telomeric repeat (2HTR, 32-bases) and from the nuclease hypersensitive region of the c-MYC gene (NHE-27, 27-bases).

Fluorescence emission spectra for **5** were obtained using a Spex Fluoromax spectrophotometer. Excitation light of 450 nm was used. Fluorescence emission spectra in the absence and presence of increasing concentrations of NHE-27 are shown in Figure 2. We performed a simple fluorescence quenching assay for both PIPER and compound **5** in the absence of DNA over the concentration range used in our experiments. Significant aggregation was noted to occur at concentrations >5 μM with both compounds (data not shown) but at the concentrations used for the titration curves with DNA (34–168 nM) no significant aggregation was observed.

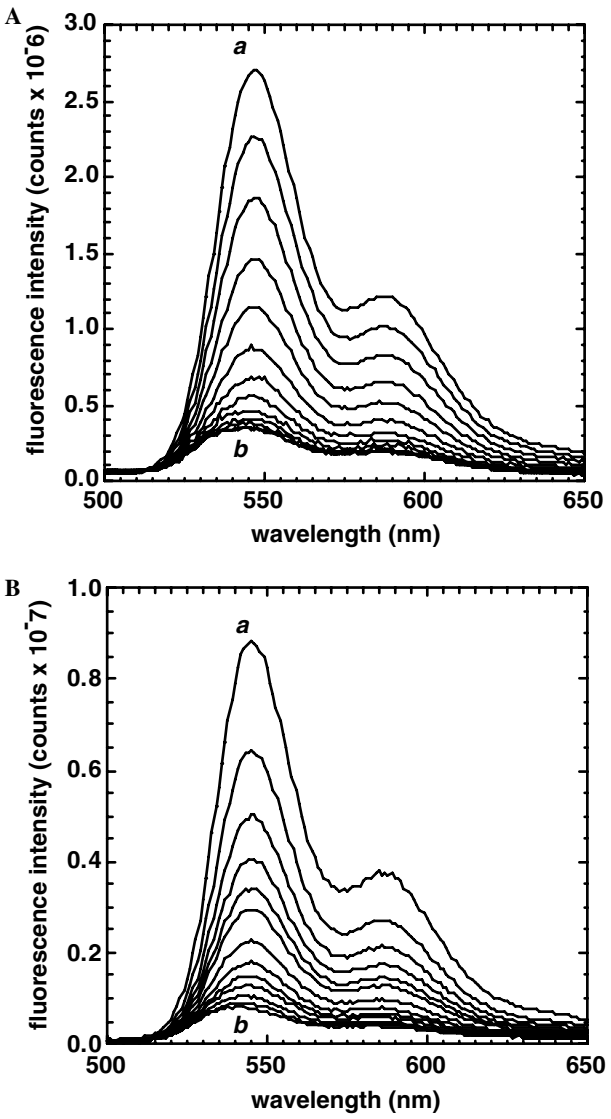

Figure 2. Binding of PIPER and **5** to single-strand DNA. The fluorescence emission spectra of (A) PIPER and (B) **5** are shown in Tris–EDTA buffer (pH 8.0) containing 100 mM KCl. The fluorescence of the perylene compounds is quenched upon binding to DNA. In both panels, curve *a* indicates initial fluorescence of the compounds (excitation at 450 nm) and curve *b* represents the final, fully bound molecules. Intervening spectra indicate the effects of addition of the G-rich ssDNA NHE-27. The quenching of fluorescence upon binding to all forms of DNA was used to determine the binding affinities of the two molecules, as shown in Figure 3.

Clearly, both PIPER and **5** bind to G-rich DNA sequences. However, the dissociation constants for the two ligands are significantly different. The quenching of fluorescence at 545 nm was used to construct the titration curves shown in Figure 3. As can be seen in Figure 3B and D, PIPER binds the single-strand NHE-27 with a K_d of $5.5 \pm 2.1 \times 10^{-9}$ M with an apparent 7 binding sites per strand. The affinity for **5** is almost 200-fold less, with a K_d of $9.8 \pm 0.3 \times 10^{-7}$ M, and all curves for **5** could be fit with a single binding site per strand. The difference between the two illustrates the effect of the cationic charge of PIPER in stabilizing the ligand–DNA complex. It also may reflect an element of steric interference from the swallowtails of **5**, which likely reduce affinity. However, the affinity of **5** is well within the range of small, uncharged molecules that bind DNA, such as actinomycin D.

PIPER binds readily to the ssDNA 2HTR as well (Fig. 3A). However, **5** does not bind this DNA to an appreciable extent (Fig. 3C) and, in fact, binds the G- and C-rich ssDNAs with low affinity equivalent to that obtained with the dsDNA formed from both strands (we estimate the K_d as $>20 \times 10^{-6}$ M). This is in contrast to PIPER, which shows a clear higher affinity for the G-rich ssDNA as well as the dsDNA formed from the two strands (Fig. 3A).

Curiously, **5** binds the dsDNA of NHE-27 weakly as compared to the G-rich NHE-27 strand alone. These means that, although the binding affinity for NHE-27 by **5** is moderate compared to cationic perylene analogs, it possesses marked selectivity toward ssDNA. This may prove useful in generating other water-soluble perylenes with greater binding affinity.

In contrast, PIPER binds with slightly higher affinity to dsDNAs of both NHE-27 and 2HTR than to the ssDNAs alone. This is likely due to the ease of intercalation into a double-stranded structure versus a quadruplex structure since at pH 8 the PIPER is less aggregated and favors dsDNA.[30] Fitting the binding curves for PIPER binding to dsDNA further suggested a simple intercalation model. The value for the number of binding sites per duplex had to be very large to effectively fit the data, and this value was fixed at 27 or 32 for NHE-27 and 2HTR, respectively. This implies approximately one base pair per binding site on the DNA, which is what would be expected with simple intercalation into the DNA structures (assuming no site exclusion). Using these values of n, the values of K_d for PIPER binding to double strand NHE-27 and 2HTR were $6.6 \pm 1.5 \times 10^{-9}$ M and $3.0 \pm 0.3 \times 10^{-8}$ M, respectively.

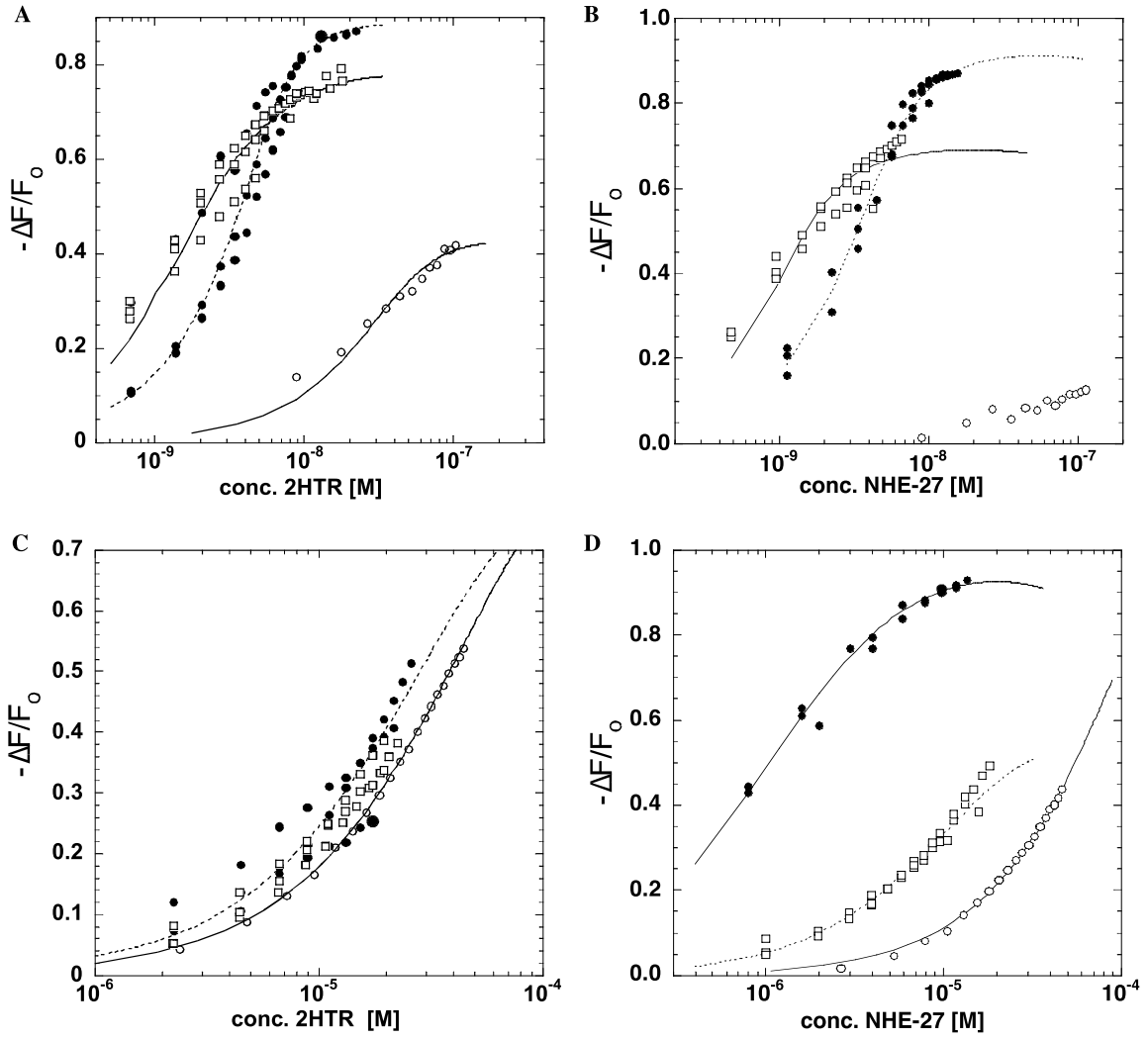

Figure 3. Affinities of PIPER and **5** to DNA. From fluorescence quenching experiments (Fig. 2), titration curves were constructed for binding of perylene analogs to different forms of DNA. In all panels, symbols are (•) G-rich ssDNA, (○) complementary C-rich ssDNA, and (□) the double stranded duplex DNA made from the two ssDNAs. Panels are: (A) PIPER binding to 2HTR, (B) PIPER binding to NHE-27, (C) **5** binding to 2HTR, and (D) **5** binding to NHE-27. Lines indicate curve fits to the simple binding model given in Eq. 1. The resulting dissociation constants (K_d) and binding sites per DNA sequence (n) are given in the text.

2.3. Non-denaturing gel electrophoresis

The perylene PIPER has been shown to drive the transition from single stranded DNA to quadruplex DNA.[11–13] We conducted similar experiments with **5** using a non-denaturing 16% polyacrylamide gel with TBE (containing KCl) as the running buffer. Concentrations of **5** were chosen according to the dissociation constants to give >90% of DNA with bound ligand at the highest concentration. As can be seen in Figure 4, while PIPER easily induces dimer and tetramer formation with increasing concentrations, compound **5** does not. PIPER can induce tetramer formation in both NHE-27 and 2HTR, and while **5** binds to the G-rich ssDNA NHE-27, it does not convert it to a dimer or tetramer. Hence, the binding seen with NHE-27 must be to the ssDNA alone. This raises the interesting possibility that uncharged perylenes bind to DNA by a mechanism that does not involve quadruplex stabilization. It will be interesting to observe how this affects telomerase activity on DNAs containing the NHE-27 sequence.

3. Conclusion

In this paper, we present the synthesis and characterization of an uncharged, water-soluble perylene compound that binds with selectivity to G-rich DNA capable of forming quadruplex structures. To our knowledge, all previously characterized perylene analogs that bind to DNA have contained side chains with substituted amino moieties, and with the exception of PIPER2 at pH > 7,[12] all have been cationic. In fact, the cationic charges are related to the selectivity of the compounds for ssDNA versus dsDNA.[11,13] As perylene analogs become deprotonated, they aggregate and selectively interact with G-rich ssDNA.

Our compound **5** is non-cationic and water soluble in its own right and shows preferential binding to the ssDNA NHE-27. While the binding affinity is lower for **5** than for the related PIPER molecule, it is still well within the range of biologically important small molecules that bind to DNA. Further, the lack of charge on **5** may

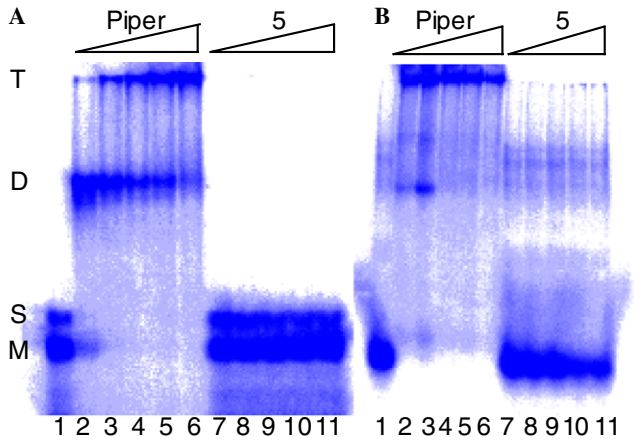

Figure 4. Induction of quadruplex structures by perylene analogs. (A) shows results for 2HTR, and (B) for NHE-27. In both panels, lane 1 indicates the G-rich ssDNA alone, while lanes 2-6 indicate increasing concentrations of PIPER and lanes 7–11 indicate increasing concentrations of compound **5**. In (A), the PIPER:2HTR ratios were 3, 6, 9, 12, and 15, and the **5**:2HTR ratios were 4.2, 8.4, 12.6, 21, and 30. In (B), the PIPER:NHE-27 ratios were 2.5, 5, 7.5, 10, and 12.5, and the **5**:NHE-27 ratios were 37, 75, 112, 149, and 186. S, M, D, and T indicate unstructured ssDNA, monomeric folded ssDNA, dimeric quadruplex, and tetrameric quadruplex, respectively. The gels and running buffer contained 100 mM KCl.

Table 2. Summary of dissociation constants (K_d) and apparent binding sites (n) for perylenetetracarboxylic diimides binding to DNA

	DNA	K_d (M)	n (sites /DNA)
PIPER	2HTR	$3.4 \pm 1.8 \times 10^{-9}$	6
	Complementary 2HTR	$1.0 \pm 0.4 \times 10^{-8}$	1
	Double-strand 2HTR	$3.0 \pm 0.3 \times 10^{-8}$	32
	NHE-27	$5.5 \pm 2.1 \times 10^{-9}$	7
	Complementary NHE-27	nd	nd
	Double-strand NHE-27	$6.6 \pm 1.5 \times 10^{-9}$	27
Compound 5	2HTR	$>20 \times 10^{-6}$	nd
	Complementary 2HTR	$>20 \times 10^{-6}$	nd
	Double-strand 2HTR	$>20 \times 10^{-6}$	nd
	NHE-27	$9.8 \pm 0.3 \times 10^{-7}$	1
	Complementary NHE-27	$>20 \times 10^{-6}$	nd
	Double-strand NHE-27	$14.8 \pm 2.1 \times 10^{-6}$	1

serve to make the molecule more easily accumulated into cells. However, compound **5** clearly does not induce formation of quadruplex DNA in the NHE-27 G-rich strand. This is in agreement with data for the weakly charged PIPER2, which also does not induce quadruplex formation. This in turn lends support to the hypothesis that the interactions of the cationic side chains with the phosphate groups of DNA are important for stabilization of quadruplexes by PIPER and related molecules.[13] Compound **5** does show excellent selectivity for G-rich ssDNA strands, despite its inability to stabilize quadruplex structures. Hence, it may form a scaffold structure for development of ssDNA-specific molecules that may be useful for affecting transcription of a number of genes.[31] Exploration of the telomerase inhibition activity of compound **5** is underway.

4. Experimental

4.1. 2-(*N*,*N*-Dibenzylamino)-1,3-propanediol (11)

Serinol (**10**, 2.00 g, 22.0 mmol) and K_2CO_3 (8.36 g, 60.5 mmol) were dissolved in 40 mL EtOH and stirred for 30 min. Afterwards, benzyl bromide (8.34 g, 48.8 mmol) was added dropwise and the reaction mixture was allowed to stir for two days at room temperature. The mixture was then filtered to remove undissolved K_2CO_3 and the filtrate was concentrated by rotary evaporation to give a white solid. This was treated with hot benzene, and the soluble portion was purified by crystallization from 25 mL of benzene and 30 mL of hexane to give white needles (5.25 g, 88%), mp 81–82 °C, R_f (silica gel, 1:1 hexane/EtOAc) 0.23. ^{1}H NMR ($CDCl_3$) δ 2.31 (s, 2H), 3.06 (m, 1H), 3.67 (m, 2H), 3.79 (m, 6H), 7.33 (m, 10H). ^{13}C NMR ($CDCl_3$ = 77.16 ppm) δ 54.1, 60.07, 60.14, 127.4, 128.7, 129.1, 139.4. Anal. Calcd for $C_{17}H_{21}NO_2$: C, 75.25; H, 7.80; N, 5.16. Found: C, 75.02; H, 7.94; N, 5.04.

4.2. *N*,*N*-Dibenzyl-2,5,8,12,15,18-hexaoxa-10-nonadecanamine (14)

NaH (1.3 g of a 60% dispersion in mineral oil, 32 mmol) was washed 3 × with 1 mL portions of hexane. Then 50 mL of THF was added to the NaH and the mixture was stirred to make a suspension. A solution of **11** (3.10 g, 11.6 mmol) in 15 mL THF was then added dropwise under nitrogen and, after 30 min of stirring, a solution of 2-methoxyethoxyethyl tosylate[32] (**13**, 6.90 g, 25.2 mmol) in 20 mL THF was added dropwise. The reaction mixture was refluxed overnight, cooled, and treated carefully with MeOH to destroy excess NaH. The solvent was removed under reduced pressure and the resulting brown oil was extracted 4× with 20 mL portions of hot ether. The combined ether fractions were concentrated by rotary evaporation to give 4.6 g (85%) of a yellowish liquid, R_f (EtOAc) 0.47. ^{1}H NMR ($CDCl_3$) δ 3.1 (m, 1H), 3.38 (s, 3H), 3.56 (m, 20H), 3.78 (s, 4H), 7.19 (m, 2H), 7.27 (m, 4H), 7.38 (m 4H). ^{13}C NMR ($CDCl_3$) δ 55.2, 56.2, 59.1, 70.4, 70.58, 70.63, 70.7, 72.0, 126.7, 128.1, 128.7, 140.8. Anal. Calcd for $C_{27}H_{41}NO_6$ 1/2 H_2O: C, 66.92; H, 8.73; N, 2.89. Found: C, 67.21; H, 8.63; N, 2.94.

4.3. 2,5,8,12,15,18-Hexaoxa-10-nonadecanamine (9)

N,*N*-Dibenzyl-2,5,8,12,15,18-hexaoxa-10-nonadecanamine (**14**, 4.00 g, 8.41 mmol) was dissolved in 110 mL MeOH and 2.5 g of 10% Pd/C catalyst was added. The mixture was hydrogenated overnight in a Parr shaker at 55 psi H_2. The reaction mixture was then filtered and the solvent was removed under reduced pressure

to give 2.01 g of an oil (81%), R_f (72:18:10 CH_2Cl_2/NH_2OH(aq)/MeOH) 0.51. ^1H NMR ($CDCl_3$) δ 2.05 (s, 2H), 3.18 (m, 1H), 3.35 (m, 8H), 3.50 (m, 6H), 3.61 (m, 12H). ^{13}C NMR ($CDCl_3$) δ 59.1, 70.48, 70.51, 70.56, 70.62, 71.9, 72.0. IR (thin film) 3522, 3364, 3290, 2891 cm^{-1}. Anal. Calcd for $C_{13}H_{29}NO_6$: C, 52.86; H, 9.90; N, 4.74. Found: C, 52.73; H, 9.93; N, 4.51.

4.4. *N*,*N*′-Di-[10-(2,5,8,12,15,18-hexaoxanonadecyl)]perylene-3,4,9,10-bis(dicarboximide) (5)

2,5,8,12,15,18-Hexaoxa-l0-nonadecanamine (**9**, 200 mg, 0.68 mmol), 3,4,9,10-perylenetetracarboxylic dianhydride (**7**, 133 mg, 0.34 mmol), imidazole (2.56 g), and $Zn(OAc)_2$ (0.03 g , 0.15 mmol) were heated at 165 °C overnight. The reaction mixture solidified upon cooling and was dissolved in MeOH. A few drops of acetic acid were added and the mixture was stirred for 15 min and then eluted through an Amberlite IR-120 (+) ion exchange column (pre-washed with water, then 2 N HCl) to remove imidazole. Lastly, imidazole-free material was obtained by column chromatography on basic alumina (0.4–0.8% MeOH in EtOAc) to give 0.09 g (28%) of deep-red solid, mp 143–144 °C, R_f (2:1 MeOH/EtOAc) 0.70. Further elution gave 0.07 g (22%) of less pure material. ^1H NMR ($CDCl_3$) δ 3.28 (s, 12H), 3.42 (m, 8H), 3.56 (m, 8H), 3.61 (m, 12H), 3.72 (m, 4H), 3.99 (m, 4H), 4.19 (m, 4H), 5.72 (m, 2H), 8.58 (m, 4H), 8.63 (m, 4H). ^{13}C NMR ($CDCl_3$) δ 52.2, 59.1, 69.4, 70.5, 70.62, 70.63, 72.0, 123.2, 123.6 (b), 126.4, 129.7, 131.7 (b), 134.6, 164.0. IR (KBr) 1700, 1654 cm^{-1}. Anal. Calcd for $C_{50}H_{62}N_2O_{16}$ 1/2H_2O: C, 62.82; H, 6.64; N, 2.93. Found: C, 62.91; H, 6.46; N, 2.93.

4.5. *N*,*N*′-Di-[10-(3,6,9-trioxadecyl)]perylene-3,4,9,10-bis(dicarboximide) (6)

3,6,9-Trioxadecylamine (90 mg, 0.55 mmol), **7** (120 mg, 0.31 mmol), imidazole (1 g), and $Zn(OAc)_2$ (catalytic amount) were combined in a reaction flask and heated to 160 °C for 18 h. The reaction mixture was then cooled to rt, stirred for 10 min with 50 mL of water, and extracted with $CHCl_3$ (3× 50 mL). The combined extracts were washed with 5% HCl (aq) to remove residual imidazole, dried over $MgSO_4$, and concentrated by rotary evaporation to give 200 mg of crude product. This was recrystallized from hexane/$CHCl_3$ to give 145 mg (77%) of **6**, R_f (9:1 $CHCl_3$/MeOH) 0.58; ^1H NMR in agreement with the literature.[17] ^{13}C NMR ($CDCl_3$) δ 39.5, 59.2, 68.0, 70.3, 70.7, 70.8, 72.0, 123.2, 123.3, 126.4, 129.4, 131.5, 134.6, 163.5. IR (KBr) 1691, 1654 cm^{-1}.

4.6. Titration curves

The DNAs used were synthesized by solid phase methods and obtained from Midland Certified Reagent Company (Midland, TX). The sequences, previously shown to be converted to quadruplex structures by small molecules,[12,33] were:

2HTR: 5′-AATCCGTCGAGCAGAGTTAGGGTTAGGGTTAG-3′

NHE-27: 5′-TGGGGAGGGTGGGGAGGGTGGGGAAGG-3′

Fluorescence quenching (Fig. 2) was used to construct the titration curves shown in Figure 3. Analogs were mixed with DNA for 2 min at 25 °C and fluorescence spectra were recorded. For PIPER, 3 mL of buffer containing 100 mM KCl, 1 mM EDTA, and 33.8 nM PIPER were titrated with G-rich ssDNA 2HTR (2.04 μM strands), the complementary C-rich ssDNA (2.04 μM strands), or duplex from mixing of the two strands (2.65 μM duplex). A similar experiment used NHE-27 (3.36 μM strands), its C-rich complementary strand (2.7 μM strands), or duplex (1.42 μM duplex). Because of potential protonation effects with PIPER, the buffer solutions were either 10 mM Tris–HCl (pH 8.0) or 200 mM MES (pH 6.5). No difference was observed between either pH.

For compound **5**, a 2.2 mL solution of 168 nM **5** in Tris–HCl buffer (10 mM) containing 100 mM KCl and 1 mM EDTA was titrated with G-rich ssDNA 2HTR (496 μM strands), the complementary C-rich ssDNA (530 μM strands), or duplex from mixing of the two strands (496 μM duplex). A similar experiment used NHE-27 (437 μM strands), its C-rich complementary strand (580 μM strands), or duplex (218 μM duplex).

Data for both compounds were recorded as $-\Delta F/F_o$, where $-\Delta F$ is the difference in fluorescence at each DNA concentration from F_o, the initial fluorescence of the drug. Fluorescence changes were fitted to the simple non-interacting site model of mass action. This model assumes a ligand (L) binds to a DNA site (D) according to:

$$L + D \rightleftharpoons LD \tag{1}$$

with a dissociation constant $K_d = ([L][D])/[LD]$. The values $[L]$, $[D]$, and $[LD]$ are molar concentrations of the free ligand, free DNA sites, and ligand-bound DNA sites, respectively. The number of sites per DNA strand is given by:

$$[D] = n[D]_o, \tag{2}$$

where $[D]_o$ is the concentration of DNA in strands or duplex and n is the number of sites per DNA. Fitting of data to the above model was done using the non-linear least squares function of Kaleidagraph (Synergy Software, Reading, PA) with K_d and $-\Delta F_{max}/F_o$ as adjustable parameters. Titrations were performed in triplicate (all data are indicated in Fig. 3), and the computed values of the parameters are reported in Table 2 for mean ± standard deviations of these triplicate determinations. For compound **5**, the number of sites per strand was fitted with $n = 1$. For PIPER, multiple binding sites were evident ($n \gg 1$), and n was fixed at 32 and 27 for double strand 2HTR and NHE-27, respectively.

4.7. Gel electrophoresis

The effects of PIPER and **5** in converting G-rich ssDNA to quadruplex structures were analyzed by non-denaturing gel electrophoresis (Fig. 4). A 16% polyacrylamide gel was used with TBE (pH 8.0) containing 100 mM KCl as the running buffer. Samples were prepared by first end-labeling 2HTR and NHE-27 with ^{32}P using T4 polynucleotide kinase, with purification of labeled DNA by spin column separation. Samples of 2HTR (1 pmol) or NHE-27 (0.9 pmol) were mixed with increasing concentrations of PIPER or **5** such that, according to the titration curves obtained, greater than 90% of the DNA had perylene analog bound to it at the highest concentration used. Ratios of PIPER:2HTR used were 0, 3, 6, 9, 12, and 15 in a 10 μL final volume. Ratios of PIPER:NHE-27 used were 0, 2.5, 5, 7.5, 10, and 12.5 in a 10 μL final volume. Ratios of **5**: 2HTR used were 4.2, 8.4, 12.6, 21, and 30 in a 10 μL final volume. Ratios of **5**: NHE-27 used were 37, 75, 112, 149, and 186 in a 10 μL final volume. Samples were incubated at 23 ± 2 °C for 4 h, then loaded onto the gel and run at 60 V at 25 °C. The resulting gel mobilities were determined by radiography.

Acknowledgments

We thank the National Science Foundation, Grants # DMR-0099674 and DBI-0421319, for financial support. The authors also thank Dr. Sean M. Kerwin, University of Texas, for providing us PIPER for these studies.

Supplementary data

Procedures for preparation of compounds **13**, **16**, and **17**. ^{1}H NMR and ^{13}C NMR spectra for **5**. Supplementary data associated with this article can be found, in the online version, at doi:10.1016/j.bmc.2006.09.075.

References and notes

1. Protozanova, E.; Macgregor, R. B. *Biochemistry* **1996**, *35*, 16638.
2. Williamson, J. R. *Annu. Rev. Biophys. Biomol. Struct.* **1994**, *23*, 703.
3. Guschlbauer, W.; Chantot, J.-F.; Thiele, D. *J. Biomol. Struct. Dyn.* **1990**, *8*, 491.
4. Kim, N. W.; Piatyszek, M. A.; Prowse, K. R.; Harley, C. B.; West, M. D.; Ho, P. L. C.; Coviello, G. M.; Wright, W. E.; Weinrich, S. L.; Shay, J. W. *Science* **1994**, *266*, 2011.
5. Sharma, H. W.; Maltese, J.-Y.; Zhu, X.; Kaiser, H. E.; Narayanan, R. *Anticancer Res.* **1996**, *16*, 511.
6. Hurley, L. H.; Wheelhouse, R. T.; Sun, D.; Kerwin, S. M.; Salazar, M.; Fedoroff, O. Y.; Han, F. X.; Han, J.; Izbicka, E.; Von Hoff, D. D. *Pharmacol. Therapeu.* **2000**, *85*, 141.
7. Hurley, L. H. *Biochem. Soc. Trans.* **2001**, *29*, 692.
8. Seenisamy, J.; Rezler, E. M.; Powell, T. J.; Tye, D.; Gokhale, V.; Joshi, C. S.; Siddiqui-Jain, A.; Hurley, L. H. *J. Am. Chem. Soc.* **2004**, *126*, 8702.
9. Siddiqui-Jain, A.; Grand, C. L.; Bearss, D. J.; Hurley, L. H. *Proc. Natl. Acad Sci. U.S.A.* **2002**, *99*, 11593.
10. Grand, C. L.; Han, H.; Munoz, R. M.; Weitman, S.; Von Hoff, D. D.; Hurley, L. H.; Bearss, D. J. *Mol. Cancer Ther.* **2002**, *1*, 565.
11. Kern, J. T.; Kerwin, S. M. *Bioorg. Med. Chem. Lett.* **2002**, *12*, 3395.
12. Rossetti, L.; Franceschin, M.; Bianco, A.; Ortaggi, G.; Savino, M. *Bioorg. Med. Chem. Lett.* **2002**, *12*, 2527.
13. Rossetti, L.; Franceschin, M.; Schirripa, S.; Bianco, A.; Ortaggi, G.; Savino, M. *Bioorg. Med. Chem. Lett.* **2005**, *15*, 413.
14. Wescott, L. D.; Mattern, D. L. *J. Org. Chem.* **2003**, *68*, 10058.
15. Demmig, S.; Langhals, H. *Chem. Ber.* **1988**, *121*, 225.
16. Metzger, R. M. *Chem. Rev.* **2003**, *103*, 3803.
17. Williams, M. E.; Murray, R. W. *Chem. Mater.* **1998**, *10*, 3603.
18. Cormier, R.; Gregg, B. *Chem. Mater.* **1998**, *10*, 1309.
19. Langhals, H. *Heterocycles* **1995**, *40*, 477.
20. Beaulieu, P. L.; Wernic, D. *J. Org. Chem.* **1996**, *61*, 3635.
21. Chandrasekhar, S.; Mohanty, P. K.; Harikishan, K.; Sasmal, P. K. *Org. Lett.* **1999**, *1*, 877.
22. The reverse Williamson is not feasible because the ditosylate of **11** is not stable. Weber, K.; Kuklinski, S.; Gmeiner, P. *Org. Lett.* **2000**, *2*, 647.
23. Benoist, E.; Loussouarn, A.; Remaud, P.; Chatal, J.-F.; Gestin, J.-F. *Synthesis* **1998**, 1113.
24. Harada, H.; Morie, T.; Hirokawa, Y.; Kato, S. *Chem. Pharm. Bull.* **1996**, *44*, 2205.
25. Langhals, H. *Chem. Ber.* **1985**, *118*, 4641.
26. Dombi, K. L.; Griesang, N.; Richert, C. *Synthesis* **2002**, 816.
27. Langhals, H.; Jona, W. *Chem. Eur. J.* **1998**, *4*, 2110.
28. Wang, W.; Li, L.-S.; Helms, G.; Zhou, H.-H.; Li, A. D. Q. *J. Am. Chem. Soc.* **2003**, *125*, 1120.
29. Li, A. D. Q.; Wang, W.; Wang, L.-Q. *Chem. Eur. J.* **2003**, *9*, 4594.
30. Kerwin, S. M.; Chen, G.; Kern, J. T.; Thomas, P. W. *Bioorg. Med. Chem. Lett.* **2002**, *12*, 447.
31. Wadkins, R. M. *Curr. Med. Chem.* **2000**, *7*, 1.
32. Weber, E. *Liebigs Ann. Chem.* **1983**, 770.
33. Rangan, A.; Federoff, O. Y.; Hurley, L. H. *J. Biol. Chem.* **2001**, *276*, 4640.